

RELATIONSHIP BETWEEN THERMAL TIDES AND RADIUS EXCESS

ARISTOTLE SOCRATES

Institute for Advanced Study, Einstein Drive, Princeton, NJ 08540
Draft version November 20, 2018

ABSTRACT

Close-in extrasolar gas giants – the hot Jupiters – display departures in radius above the zero-temperature solution, the radius excess, that are anomalously high. The radius excess of hot Jupiters follows a relatively close relation with thermal tidal torques and holds for $\sim 4 - 5$ orders of magnitude in a characteristic thermal tidal power in such a way that is consistent with basic theoretical expectations. The relation suggests that thermal tidal torques determine the global thermodynamic and spin state of the hot Jupiters. On empirical grounds, it is shown that theories of hot Jupiter inflation that invoke a constant fraction of the stellar flux to be deposited at great depth are, essentially, falsified.

Subject headings: planets: hot Jupiters

1. INTRODUCTION

The radii of hot Jupiters are anomalously larger than their zero temperature radii, R_0 (Bodenheimer et al. 2003; Arras & Bildsten 2007). The powerful stellar radiation field serves as an ample source of energy which may inflate hot Jupiters to their current radii (Guillot & Showman 2002). The major theoretical challenge is in finding a mechanism that can transfer a small amount ($\lesssim 1\%$) of the stellar insolation to great depth. Current ideas include thermal tides (Arras & Socrates 2009a,b; 2010), delayed gravitational contraction (Ibgui et al. 2010) and ohmic dissipation due to magnetic activity on the heavily irradiated surface (Batygin & Stevenson 2010).

It seems that there is an relation between observed radius excess Δ defined as

$$\Delta \equiv \frac{R_p - R_0}{R_p},$$

where R_p is the measured planet radius, and a characteristic thermal tidal power L_{thT} defined as

$$L_{\text{thT}} \equiv \frac{\sigma_{\text{SB}}}{c_p} n^2 T_{\text{eq}}^3 R_p^4$$

where σ_{SB} is the Stefan-Boltzmann constant, c_p is the specific heat, n is the mean motion and T_{eq} is its equilibrium surface temperature.

The radius excess Δ is determined by a balance of heating and cooling. In the thermal tide scenario, the thermal tide torque is balanced by the gravitational torque. While the thermal tide torque is non-dissipative, the gravitational tide torque necessarily is the result of dissipation. Torque balance in steady state then implies continuous heating as a result of gravitational tidal dissipation. It follows that the planet radius is determined by a balance of this steady state heating with cooling at the photosphere. The ultimate source of energy is the stellar radiation field, which performs work by moving material across the tidal potential, near the surface of the irradiated planet (Arras & Socrates 2009a; 2010).

The plan of this paper is as follows: In §2 we motivate the need for thermal tidal torques in hot Jupiters, compute their characteristic values for both equilibrium and

dynamical thermal tides as well as the the characteristic thermal tidal power, all in terms of physical quantities that can be observationally inferred. The thermal tide - radius excess relation is presented in §3. A brief discussion is contained in §4. A brief summary is given in §5.

2. THEORY OF THERMAL TIDES IN HOT JUPITERS

The radiation field of a star forces the atmospheres of planets in orbit. The response of a planetary atmosphere to this forcing is referred to as the “thermal tide.” Planets that spin asynchronously experience a sharp change in thermal forcing during twilight hours and consequently, a broad spectrum of tidal harmonics are excited. For circular orbits, the semi-diurnal ($\ell = m = 2$) harmonic of the forcing leads to a thermal tidal bulge that can couple to the leading order term of the gravitational tidal potential. The atmosphere’s finite thermal inertia leads to a lag in the response with respect to the forcing, which allows the tidal potential to exert a net torque on the thermal tide during the heating cycle. Since the thermal tidal bulge peaks in the morning and after sunset, but before midnight, the acceleration increases the planet’s rotational energy.

The picture described above has a long history. On the basis of the measured magnitude and phase of Earth’s thermal tide, Thompson (Lord Kelvin) computed Earth’s thermal tidal torque and found it to be approximately equal to one tenth the dissipative lunar tidal torque (Thompson 1882; see also Munk & Macdonald 1960). Due to its heavy atmosphere and correspondingly large thermal tides, Gold & Soter (1969) hypothesized that the current spin state of Venus results from a balance of thermal and gravitational tidal torques so that its current state of spin can be maintained over the age of the solar system.

In what follows, we motivate the importance of thermal tides and thermal tidal torques in hot Jupiters, within the context of understanding their inflated radii.

2.1. tidal power as a source of dissipation

The characteristic value for the maximum instantaneous tidal power for a uniform spherical body of radius

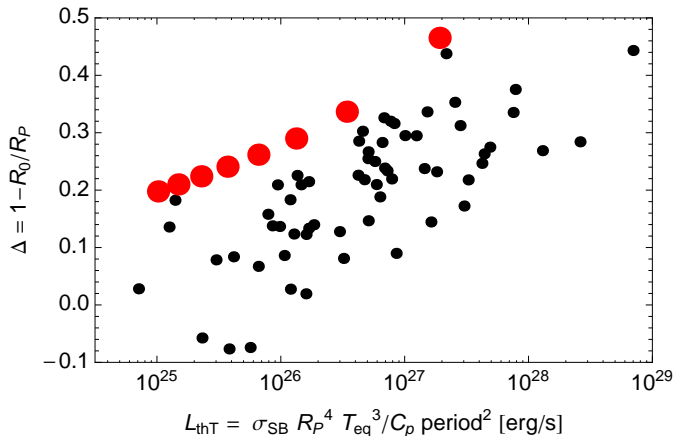


FIG. 1.— The $\Delta - L_{\text{thT}}$ relation for a sample of 63 hot Jupiters with $M \sin i > 0.5 M_J$. An approximation for the zero temperature radius R_0 is obtained by using the cooling models of Baraffe et al. (2010) for core-less planets with $Z = 0.02$ in the absence of irradiation at an age of 7 Gyrs. Large red points are theory, computed using the Gold-Soter approximation for a Jupiter-mass, core-less $Z = 0.02$ planet whose optical absorption opacity $\kappa_* = 0.003$ (Arras & Socrates 2009a). The tidal quality factor of the planet is chosen such that $Q = 10^5$ for the Jupiter-Io interaction and the constant lag time model of Hut (1981) is employed in order to compute the gravitational tidal torque and equilibrium dissipation rate.

R in a Keplerian orbit about a central source of mass M at a heliocentric distance D is given by

$$L_{\text{max,T}} \approx \frac{c_{\text{T}}^5}{G} \quad (1)$$

where the characteristic tidal speed c_{T} is given by

$$c_{\text{T}} \equiv R \sqrt{\frac{GM}{D^3}} \quad (2)$$

and G is Newton's constant¹. The expression above is obtained by taking the peak energy of the equilibrium tidal response to dissipate with a timescale given by the inverse of $\sqrt{GM/D^3}$.

Most hot Jupiters are in nearly circular orbits. In that case, $n = \sqrt{GM/a^3}$ is the mean motion and only the synchronization tide can lead to tidal dissipation and therefore, the forcing frequency is given by the difference of the spin frequency and mean motion. If the planet is rapidly spinning such that the characteristic tidal forcing frequency in eq. 1 is taken to be the mean motion n , then eq. 1 may be written as

$$L_{\text{max,T}} \approx 10^{34} P_3^{-5} R_{10}^5 \quad (3)$$

where P_3 is the orbital period P_{orb} in units of 3 days and R_{10} is the planet's radius, R_p , normalized to 10^{10} cm. The power required to maintain the radii of heavily inflated hot Jupiters is of order $\approx 10^{28}$ erg/s and therefore, only a small fraction of the total available tidal power is required to produce inflated hot Jupiters in steady-state.

¹ Note the similarity of eq. 1 with maximum luminosity of any object in the Universe

$$L_{\text{max}} = \frac{c^5}{G}.$$

2.2. the role of thermal tides

Stellar irradiation creates a tidal bulge that leads maximum forcing at noon, where the phase shift results from thermal inertia. The tidal gravitational field of the star torques the thermal tide, accelerating the planet away from a state of synchronous spin. As the rate of spin increases, the amount of energy absorbed per cycle decreases and consequently, so does the magnitude of the thermal tidal quadrupole. The thermal tide torque eventually comes into balance with the usual dissipative gravitational tidal spin-down torque. In steady-state, the planet's spin is asynchronous and therefore, gravitational tidal power is continuously dissipated. The ultimate source of energy is the starlight of the primary, which performs work by moving material across the tidal potential (Arras & Socrates 2009a; 2010).

A fundamental underlying assumption of this picture is that dissipation of the gravitational tide takes place at great depth, where the pressure scale height is comparable to the radius of the planet.

Also note that, in the absence of thermal tidal torques, gravitational tidal torques are likely to synchronize the planet spin extremely fast if the relative strength of tidal dissipation in hot Jupiters is comparable to what is commonly inferred from the Jupiter-Io interaction (Goldreich & Soter 1966; Socrates et al. 2012).

2.3. spin equilibrium and steady tidal power: Gold-Soter approximation

Balance between the gravitational tidal torque and the thermal tidal torque determines the planet's spin rate and therefore, determines the tidal forcing frequency ω . For a circular or nearly circular orbit, torque balance is obtained by equating the respective quadrupoles induced by thermal and gravitational forcing. The portion of the gravitationally excited quadrupole responsible for dissipation and secular evolution is given by

$$q_{\text{grav}} = \frac{n^2 R_p^5}{Q_J \omega_J G} \quad (4)$$

where the above expression for the tidal quality factor Q reflects the frequency dependence of the constant lag time model of Hut (1981). Here Q_J and ω_J is the tidal quality factor ($\approx 10^5$; Goldreich & Soter 1966) and forcing frequency (≈ 10 hours) of the Jupiter-Io interaction. Note that we are, equivalently, setting the lag time $\tau \approx 0.1$ s, consistent with the resonant configuration of the Galilean satellites (Socrates et al. 2012; Leconte et al. 2010; see also Socrates & Katz 2012).

The Gold-Soter quadrupole due to thermal forcing is approximately given by

$$q_{\text{th}}^{\text{GS}} = \frac{\Delta M R_p^2}{t_{\text{th}} \omega} = \frac{\sigma_{\text{SB}} R_p^4 T_{\text{eq}}^3}{c_p \omega} \quad (5)$$

where ΔM and t_{th} are the mass and thermal relaxation time, respectively, of the absorbing layer and t_{th} . In terms of physical quantities, the thermal time may be written as

$$t_{\text{th}} \equiv \frac{c_p}{\sigma_{\text{SB}}} \frac{\Delta M}{R_p^2 T_{\text{eq}}^3}. \quad (6)$$

By equating eq. 4 with eq. 5, the equilibrium forcing frequency becomes

$$\begin{aligned} \omega_{\text{GS}} &= \sqrt{\frac{\sigma_{\text{SB}} Q_{\text{J}} \omega_{\text{J}}}{c_p} \frac{T_{\text{eq}}^3}{n^2 R_p}} \\ &\approx \frac{2\pi}{2 \text{ days}} T_{2000}^{3/2} P_4 R_{10}^{-1/2} Q_5^{1/2} \end{aligned} \quad (7)$$

where T_{2000} , P_4 , R_{10} , Q_5 are the equilibrium temperature in units 2000 K, the orbital period normalized to four days, dimensionless planet radius normalized to 10^{10} cm and the tidal quality factor of the Jupiter-Io interaction, normalized to 10^5 .

In the equilibrium – Gold-Soter – approximation, the tidal dissipation rate resulting from the balance of thermal and gravitational tidal torques, which we refer to as the thermal tidal power $L_{\text{thT}}^{\text{GS}}$ is given by

$$\begin{aligned} L_{\text{thT}}^{\text{GS}} &= \omega_{\text{GS}} n^2 q_{\text{grav}} = \omega_{\text{GS}}^2 \frac{n^4 R_p^5}{G Q_{\text{J}} \omega_{\text{J}}} \\ &\approx \frac{\sigma_{\text{SB}}}{c_p} n^2 T_{\text{eq}}^3 R_p^4 \\ &= 1.5 \times 10^{28} P_4^{-2} T_{2000}^3 R_{10}^4 \text{ erg/s.} \end{aligned} \quad (8)$$

2.4. spin equilibrium and steady tidal power: dynamical thermal tides

Consider the computed thermal tide quadrupole from Arras and Socrates (2010; see their figure 5) for the case with outgoing radiation boundary condition. We imagine an evolutionary scenario in which the planet was born spinning rapidly and was then placed in its current orbit via some migration mechanism. As it spins down, the forcing frequency approaches the g-mode ‘‘bump’’ in the thermal tidal quadrupole, which is responsible for arresting any further spin evolution. The first spin up feature of the g-mode bump is located near the cutoff frequency ω_0

$$\omega_0 = \frac{H}{R_p} N \quad (9)$$

where H is scale height of the isothermal layer that lies above the convection zone and N is the Brunt-Vaisalla frequency, the characteristic rate at which the buoyancy force restores motion.

It is worth noting that the cutoff frequency ω_0 is close to the mean motion n of hot Jupiters. If $\omega_0 \ll n$, the quadrupole moments associated with low radial order gravity waves would be small and therefore, so would the quadrupole of the thermally-forced response. From this perspective, it is somewhat of a co-incidence that dynamical thermal tides in the hot Jupiters can lead to significant spin-up tidal torques.

The spin-up quadrupole due to the first feature in the g-mode bump may be expressed as

$$q_{\text{th}}^g = q_{\text{th}}^{\text{GS}}(\omega = \omega_0) f(\omega, \omega_0) \quad (10)$$

where f can be approximated by a sharply-peaked Gaussian of the form

$$f(\omega, \omega_0) \simeq \beta e^{-(\omega - \omega_0)^2 / \Gamma^2} \quad (11)$$

where $\beta \approx 0.1$ quantifies the amount by which gravity waves near the cut-off frequency do not perfectly overlap

with both thermal and gravitational forcing. The width of the Gaussian is narrow so that $\Gamma \ll \omega_0$.

Spin equilibrium is determined by setting $q_{\text{th}}^g = q_{\text{grav}}$, which gives

$$e^{-(\omega - \omega_0)^2 / \Gamma^2} \simeq \left[\frac{c_p}{\sigma_{\text{SB}} G} \frac{n^2 R_p \omega_0^2}{\beta T_{\text{eq}}^3 Q_{\text{J}} \omega_{\text{J}}} \right] \frac{\omega}{\omega_0}. \quad (12)$$

The right hand side must be less than unity in order for torque balance to be satisfied. For the physical parameters that describe the hot Jupiter population, torque balance is only possible for $Q_{\text{J}} \gtrsim 10^5$. If there is some level of sub-surface reflection the excited gravity waves are quantized and their response is therefore, characterized by a Lorentzian profile near resonance, implying that the induced quadrupolar response can be much larger. Consequently, values of $Q_{\text{J}} \approx 10^4$ or $\tau \simeq 1$ s are then possible for a steady-state spin equilibrium (Arras & Socrates 2010).

Due to the sharpness of the Gaussian, the forcing frequency in spin equilibrium, given by eq. 12, is pinned to a value that is close to the cutoff frequency

$$\omega \approx \omega_0. \quad (13)$$

By following the steps in eq. 8, a similar expression for thermal tidal power, $L_{\text{thT}}^{\text{dyn}}$ is derived due to the presence of dynamical tides

$$L_{\text{thT}}^{\text{dyn}} \approx 1.2 \times 10^{28} \omega_2^2 P_4^{-4} R_{10}^5 Q_5^{-1} \text{ erg/s} \quad (14)$$

where ω_2 and Q_5 are the semi-diurnal forcing frequency normalized to $(2\pi/2 \text{ days})$ and the tidal quality factor of the Jupiter-Io interaction, normalized to 10^5 .

The thermal tidal dissipation rate, eq. 14 resulting from the dynamical excitation of gravity waves, is similar in form and magnitude to that resulting from the Gold-Soter approximation, given by eq. 8. From here on, when comparing with data, we employ the Gold-Soter approximation since (i) it is simple (ii) in terms of spin equilibrium and persistent tidal luminosity, it roughly agrees with the more realistic dynamical tide results of Arras & Socrates (2010) (iii) the theory of dynamical thermal tides is currently in a state of development.

3. THERMAL TIDE-RADIUS EXCESS RELATION

The fractional radius anomaly Δ , given by

$$\Delta \equiv 1 - R_0 / R_p, \quad (15)$$

where R_0 is a fiducial radius that is close the zero temperature solution depends upon planet mass and composition. The value for R_0 is obtained by using the online table provided by Baraffe et al. (2008) by choosing choosing $Z = 0.02$ with no irradiation and their largest computed age of 7 Gyr.

The primary reason for utilizing the models of Baraffe et al. for the values of R_0 , rather than the actual zero temperature or isothermal radius is that they are publicly available. Their solutions serve as a fiducial value of low planetary entropy that depends on planet mass. It follows that any observed departure in planet radius R_p above R_0 necessitates a source of thermal energy from within the planet.

The sample of hot Jupiters is taken from the Exoplanet Data Explorer, located on the world wide web. Only hot Jupiters with measured mass, radius, effective temperature and orbit that have measurements i.e., a sizable

fraction of the total sample, are considered. Furthermore, the sample is limited to hot Jupiters with masses $M > 0.5M_J$. All of the planets considered have both transit and radial velocity measurements, for a total of 63 objects.

In figure 1 we plot radius anomaly Δ against the dissipation rate given by eq. (8). There is a clear relationship. Any level of deep internal energy generation increases the central entropy, lifts the degeneracy and expands the planetary radius. Figure 1 indicates that the radius anomaly, or departure from the zero temperature radius, increases with an increasing internal dissipation rate that is correlated to the characteristic thermal tidal dissipation rate L_{thT} . That is, figure 1 lends strength to the hypothesis that thermal tidal torques power the core luminosities of hot Jupiters.

Figure 1 implies that radius excess Δ , rather than planet radius R_p is more sensitive in ascertaining the actual internal luminosity of a given planet and is therefore, a more useful parameter. The reason for this is straightforward: the mass-radius relation of cold spheres (e.g., Zepolsky & Salpeter 1969) indicates that – for a fixed composition – radius is approximately independent of mass. Thus, the gravitational binding energy and approximately, the Fermi energy, vary by nearly two orders of magnitude. As a result, the energy and power requirements to lift the degeneracy and inflate the radius are far more severe for massive objects. The relatively small scatter in figure 1 in comparison to similar figures that utilize planet radius (e.g., figure 1 of Demory & Seager 2011; figure 1 of Laughlin et al. 2011; figure 1 of Fortney et al. 2011) is partially due to this fact.

4. DISCUSSION

Figure 1 is important irrespective of whether or not it supports the thermal tide model of Arras & Socrates. It indicates that the internal luminosity of the hot Jupiters varies by $\sim 4 - 5$ orders of magnitude. Such a conclusion can be indirectly inferred from e.g., recent work by Spiegel & Burrows (2013), independent of the actual source of thermal power at great depth.

With the exception of the thermal tide scenario advocated here, nearly every plausible model of steady-state hot Jupiter inflation invokes or presumes some fixed fraction of absorbed stellar energy to be redistributed to great depth (e.g., Guillot & Showman 2002; Batygin & Stevenson 2010; Youdin & Mitchell 2012; Laughlin et al. 2012). The stellar flux varies like $1/D^2$ and therefore, so does – for fixed planet radius and stellar type – the available amount of energy absorbed. Largely due to the fact that hot Jupiters – by definition – possess orbital separations $0.01\text{AU} \leq D \leq 0.1\text{AU}$, the spread in the available energy in starlight varies by approximately two orders of magnitude. Since the observed spread in radii requires a corresponding spread in steady state power of $\sim 4 - 5$ orders of magnitude, theories that utilize a

constant fraction of the absorbed stellar light are then, effectively, falsified.

In general, the amplitude of a tidal response is $\propto 1/D^3$ and therefore, the energy in the tidal interaction, which is proportional to the square of the tidal amplitude, is $\propto 1/D^6$. For the case of thermal tides, the tidal response is forced by the stellar radiation flux and is therefore $\propto 1/D^2$. The tidal interaction, which leads to orbital and spin evolution, is given by the product of the thermal tide quadrupole and the tidal potential and is thus $\propto 1/D^5$. Consequently, the expected spread in thermal tidal power for the hot Jupiters is roughly 5 orders of magnitude, consistent with what is required to inflate their radii.

The hot Jupiters sit deep within a steep tidal potential ($\propto 1/D^3$) that leads to even more rapidly varying tidal interaction potentials ($\propto 1/D^6$ for gravitational tides and $\propto 1/D^5$ thermal tides). Relatively modest displacements in orbital separation leads to relatively large changes in the internal tidal luminosity. In a way, the radius excess phenomena displayed by the hot Jupiters can be thought of as a manifestation of, otherwise degenerate, gaseous self-gravitating bodies probing deep and rapidly varying interaction potentials.²

5. SUMMARY

An observed relationship between radius excess Δ and a characteristic thermal tidal power L_{thT} for the hot Jupiters is given in figure 1. It indicates that, in order to produce the observed trend in radius excess Δ , the internal luminosity must vary by $\sim 4 - 5$ orders of magnitude for the population of inflated hot Jupiters. This empirical requirement lends support to *any* tidal scenario that inflates the hot Jupiters steadily over the age of the Galaxy and therefore, lends support to the steady-state thermal tide scenario of Arras & Socrates (2009a; 2010).

Furthermore, the empirical requirement that a large spread of inferred internal luminosity is required to explain the trend in radius excess Δ from figure 1 falsifies theories of hot Jupiter inflation that invoke, presume or calculate that a fixed fraction of the absorbed stellar power is transferred to great depths.

Both equilibrium and dynamical thermal tides approximately yield comparable values for equilibrium thermal tidal power and planetary spin rate. The role of thermal tides can be viewed as allowing for the steady dissipation of tidal energy that is continuously replenished by the stellar radiation field as it performs work by moving matter across the tidal potential (Arras & Socrates 2009a; 2010).

I thank P. Arras for extensive conversations and for assistance. Subo Dong, Andy Gould and Scott Tremaine provided helpful suggestions. AS acknowledges support from a John N. Bahcall Fellowship at the Institute for Advanced Study, Princeton.

REFERENCES

- Applegate, J. H., & Shaham, J. 1994, ApJ, 436, 312
 Arras, P., & Bildsten, L. 2006, ApJ, 650, 394
 Arras, P., & Socrates, A. 2009, arXiv:0901.0735
 Arras, P., & Socrates, A. 2009, arXiv:0912.2318
 Arras, P., & Socrates, A. 2010, ApJ, 714, 1
 Baraffe, I., Chabrier, G., & Barman, T. 2008, A&A, 482, 315
 Batygin, K., & Stevenson, D. J. 2010, ApJ, 714, L238
 Bodenheimer, P., Laughlin, G., & Lin, D. N. C. 2003, ApJ, 592, 555
 Demory, B.-O., & Seager, S. 2011, ApJS, 197, 12
 Fortney, J. J., Demory, B.-O., Désert, J.-M., et al. 2011, ApJS, 197, 9
 Fruchter, A. S., Stinebring, D. R., & Taylor, J. H. 1988, Nature, 333, 237

- Gold, T., & Soter, S. 1969, *Icarus*, 11, 356
Goldreich, P., & Soter, S. 1966, *Icarus*, 5, 375
Guillot, T., & Showman, A. P. 2002, *A&A*, 385, 156
Hut, P. 1981, *A&A*, 99, 126
Ibgui, L., Spiegel, D. S., & Burrows, A. 2011, *ApJ*, 727, 75
Laughlin, G., Crismani, M., & Adams, F. C. 2011, *ApJ*, 729, L7
Leconte, J., Chabrier, G., Baraffe, I., & Levrard, B. 2010, *A&A*, 516, A64
Munk, W. H., & MacDonald, G. J. F. 1960, Cambridge [Eng.] University Press, 1960.,
Spiegel, D. S., & Burrows, A. 2013, arXiv:1303.0293
Socrates, A., Katz, B., & Dong, S. 2012, arXiv:1209.5724
Socrates, A., & Katz, B. 2012, arXiv:1209.5723
Thompson, W. 1882, *Proc. Roy. Soc. Edinburgh* 11, 369
Youdin, A. N., & Mitchell, J. L. 2010, *ApJ*, 721, 1113
Zapolsky, H. S., & Salpeter, E. E. 1969, *ApJ*, 158, 809

This figure "framework.png" is available in "png" format from:

<http://arxiv.org/ps/1304.4121v1>